2009 American Control Conference
Hyatt Regency Riverfront, St. Louis, MO, USA
June 10-12, 2009

Model-Based Engine Fault Detection and Isolation

Arkadiusz Dutka[¶], Hossein Javaherian[§] and Michael J. Grimble[†]

***Abstract*— To a large extent, tailpipe emissions are influenced by the accuracy and reliability of the intake manifold sensors and the predictive models used for cylinder charge estimation. In this paper, mathematical models of an internal combustion engine are employed to detect failures in the intake manifold. These can be associated with the upstream sensors such as the pressure and temperature sensors as well as systemic faults such as a leakage in the intake manifold. Any fault will adversely affect the proper operation of the air-fuel ratio control system and must be detected at an early stage. Through the use of dedicated observers, residual errors can be generated and thresholds established. Methods for the isolation of the detected faults are proposed and applied to a 5.7 L V8 engine model. Simulation results for the Federal Test Procedure (FTP) driving cycle indicate that fast and reliable detection and isolation of the faults is possible.**

I. Introduction

Fault detection in combustion engines has been the subject of a number of investigations [1], [2], [3]. Current production systems are based mainly on the simple limit and plausibility checks of measured signals. Some simple signal-based methods like frequency based analysis methods are also employed [4]. Stringent demands on the detection speed and the ability to accurately pinpoint the source of a fault require more rigorous techniques. In addition, the current On-Board Diagnostics II (OBDII) systems may not be capable of detecting relatively small offsets and drifts of the sensor data. In the following we will concentrate on the "intake manifold" fault detection problem to demonstrate the capabilities of the proposed model-based estimation, method coupled with a physical analysis of the system.

The analysis of the intake manifold system has been considered earlier in [5] and [6]. The hypothesis testing framework based on the system model was used for the intake manifold leaks and sensor faults detection. In the following the non-linear observer-based fault detection for the intake manifold is considered. The fault detection, isolation and identification are carried out based on a generalized observer approach.

The faults appearing in the system are modeled as additive signals. The intake manifold pressure and the temperature sensor faults are modeled as additive perturbations. The intake manifold leak is modeled by one-dimensional flow equations in a similar way to the throttle flow. The product of the leakage area and the discharge coefficient is defined as the unknown input f_{leak}. The pressure sensor fault $f_{P_{im},n}$ is modeled as an additive saturated ramp signal. The temperature fault $f_{T_{im,meas},n}$ is also modeled in the same way as an additive signal. These changes simulate the measurement offset. In practice, a common situation is when the sensor is stuck, which may also be simulated by the time-varying additive signal. The intake manifold leak is assumed to appear more abruptly. This may be seen as a vacuum hose being pulled off the intake manifold. The leak area will be assumed to be constant.

In this work it is assumed that faults do not appear simultaneously. Also, the electronic throttle is assumed to be equipped with redundant position sensors and consequently the fault diagnosis may be based on the physical redundancy within its dedicated control system. Simulation results use data obtained from a real vehicle as inputs and external parameters. The analysis is limited to the simulations of the proposed methodologies on the FTP driving cycle transients.

II. Residuals Generation – Dedicated Observer Scheme

The most important task in fault detection lies in the residual generation. In the system diagram in Fig. 1, faults consist of two sensor faults and one system fault represented by the intake manifold leak. Sensor faults are modeled as additive signals on outputs. The system fault is modeled as an unknown input to the system.

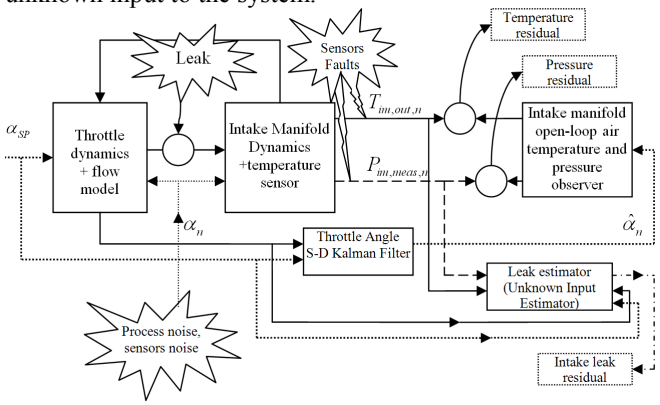

Fig. 1: System faults and a dedicated estimator scheme

A. The system model

The model of Fig. 1 for an 8-cylinder (V8) engine is discretized using an "event-based" sampling rate of 90º crank angle. This implies that the sampling period varies with the engine speed. In an event-based sampling of the engine model, the variable sampling period is given by $T_{s,n} = 120/8N_n\,[s]$, where N_n is the engine speed in

Manuscript received 15 August 2008. This work was supported by the General Motors Corporation. ¶ A. Dutka is with ISC Ltd, Glasgow, UK (arkadiusz.dutka@strath.ac.uk), § H. Javaherian is with GM R&D, Warren, MI, USA, (hossein.javaherian@gm.com) † M. J. Grimble is with the University of Strathclyde, Glasgow, UK (m.grimble@eee.strath.ac.uk).

revolutions per minute at the discrete event *n*. The first part of the overall model is first defined: that is the electronic throttle model is given by the following state-space equations [7], [8]:

$$\begin{aligned} x_{ET,n+1} &= A_{ET}(N_n)x_{ET,n} + B_{ET}(N_n)\alpha_{SP,n} + w_{ET,n} \\ \alpha_n &= C_{ET}x_{ET,n} + v_{ET,n} \end{aligned} \quad (1)$$

where $x_{ET,n}$ is the throttle state vector, $\alpha_{SP,n}$ is the angle setpoint signal and α_n is the indicated throttle angle. System matrices are non-linear functions of the engine speed.

The intake manifold is modeled by the following non-linear state-space system:

$$\begin{aligned} x_{IM,n+1} &= f\left(x_{IM,n}, \alpha_n, f_{leak,n}, N_n\right) + w_{EM,n} \\ y_{IM,n} &= C_{IM}x_{IM,n} + f_{IM,n} + v_{EM,n} \end{aligned} \quad (2)$$

where $x_{IM,n}$ is the state vector, $f_{leak,n}$ is the product of the leak area and the discharge coefficient for one-dimensional flow through the orifice, $w_{EM,n}$ is the intake manifold process noise, $f_{IM,n} = \begin{bmatrix} f_{P_{im},n} & f_{T_{im},n} \end{bmatrix}^T$ is the sensor faults vector with the intake manifold pressure sensor fault and air temperature sensor fault, $v_{EM,n}$ is the intake manifold pressure measurement noise and $y_{IM,n} = \begin{bmatrix} P_{im,meas,n} & T_{im,meas,n} \end{bmatrix}$ is the vector of pressure and temperature measurements.

The intake manifold model is parameterized in a state-dependent form and augmented with the throttle model [8]:

$$\begin{aligned} x_{n+1} &= A_n\left(x_n\right)x_n + B_n\left(x_n\right)u_n + F_n\left(f_{leak,n}\right)f_{leak,n} + w_n \\ y_n &= C_n x_n + f_{S,n} + v_n \end{aligned} \quad (3)$$

where

$u_n = TA_{SP,n}$, $x_n = \begin{bmatrix} x_{ET,n}{}^T & x_{IM,n}{}^T \end{bmatrix}^T$, $f_{S,n} = \begin{bmatrix} 0 & f_{IM,n}{}^T \end{bmatrix}^T$,

$y_n = \begin{bmatrix} TA_n & y_{IM,n}{}^T \end{bmatrix}^T$, $w_n = \begin{bmatrix} w_{ET,n}{}^T & w_{IM,n}{}^T \end{bmatrix}^T$,

$v_n = \begin{bmatrix} v_{ET,n}{}^T & v_{IM,n}{}^T \end{bmatrix}^T$.

Note that the throttle position sensor fault is not considered here due to physical redundancy present in modern electronic throttle actuators. w_n and v_n are independent white Gaussian noise signals with $\mathrm{cov}\{w_n\} = Q$ and $\mathrm{cov}\{v_n\} = R$. Q and R are diagonal semi-positive and positive definite matrices, respectively. An identification of the stochastic properties of the system based on real vehicle data was carried out to obtain matrices Q and R representing noise magnitudes.

B. Sensor faults directional residuals generation

Each dedicated observer uses the throttle angle setpoint command α_{SP}, the throttle angle measurement α_n and either the temperature $T_{im.meas,n}$ or the pressure $P_{im,meas,n}$ measurement. Each observer carries out diagnosis of only one output signal that may be the subject of fault. This provides the isolation of each individual estimator. The intake air temperature sensor estimator detects the temperature sensor fault and is not sensitive to the pressure sensor fault. Similarly the intake air pressure sensor estimator detects the pressure sensor fault and is insensitive to the temperature sensor fault. Under the hypothesis that the intake manifold leak is not present, the sensor fault detection may be established through the analysis of residuals which are the differences between the estimated and the measured outputs generated by each estimator.

For the throttle angle estimation, a separate *state-dependent Kalman filter* was designed (see Fig. 1). The throttle angle estimate is used by the open-loop observer to compute the intake manifold pressure and temperature. The non-linear closed loop estimator (e.g. state-dependent Kalman filter) requires state estimates for the model update. In the presence of an additive sensor fault the state estimates will diverge from the actual system state values. This may be demonstrated using the following equation:

$$\begin{aligned} \hat{x}_{n+1} = &\left(\hat{A}_n - \hat{A}_n K_n \hat{C}_n\right)\hat{x}_n + \hat{A}_n K_n C_n x_n + \\ &\hat{A}_n K_n f_{S,n} + \hat{A}_n K_n v_n + \hat{B}_n u_n \end{aligned} \quad (4)$$

The matrix K_n is a Kalman gain obtained from the solution of the discrete algebraic equation computed for the system matrices frozen at the current state. The senor fault $f_{S,n}$ which is assumed to have a non-zero mean value acts as an additional unknown input to the estimator resulting in the state estimation offset. This offset will result in the discrepancy between the model matrices: $\hat{A}_n = \hat{A}\left(\hat{x}_n\right)$, $\hat{B}_n = \hat{B}\left(\hat{x}_n\right)$, $\hat{C}_n = \hat{C}\left(\hat{x}_n\right)$ and the actual system matrices $A_n = A\left(x_n\right)$, $B_n = B\left(x_n\right)$, $C_n = C\left(x_n\right)$. The discrepancy depends on the particular system non-linearity for which a general analysis is not available. For linear systems with constant matrices, model mismatch does not occur due to this cause. In closed-loop operation, this results in an improved estimation. The same effect is not guaranteed for general non-linear systems. The state-dependent Kalman filter error signal generated for *i-th* output and used as the residual is given by the following expression:

$$r_{i,n} = C_n x_n - \hat{C}_n \hat{x}_n + f_{S,n} + v_n \quad (5)$$

The residual $r_{i,n}$ will directly reflect the sensor fault $f_{S,n}$. Unfortunately, the past values of the fault signal $f_{S,n}$ are also present in the state estimate $\hat{x}_n$ (see equation (4)). This results in rather unpredictable response of the residual $r_{i,n}$ to the fault $f_{S,n}$. This is due to the non-linear characteristics of the system and the state-dependent model mismatch may have a negative effect on the residual signal sensitivity to the fault. This negative influence is caused by the state estimate $\hat{x}_n$ bias and the model matrix $\hat{C}_n$ mismatch. However, these effects are absent if the open-loop system is used.

Extensive simulations of the open-loop stable intake manifold indicate that the direct use of the non-linear system model provides improved results. The state of the system in open-loop may be obtained using the following equation:

$$\hat{x}_{OL,n+1} = \hat{A}_{OL,n}\hat{x}_{OL,n} + \hat{B}_{OL,n}u_n \quad (6)$$

where

$\hat{A}_{OL,n} = \hat{A}\left(\hat{x}_{OL,n}\right)$, $\hat{B}_{OL,n} = \hat{B}\left(\hat{x}_{OL,n}\right)$ and $\hat{C}_{OL,n} = \hat{C}\left(\hat{x}_{OL,n}\right)$.

The state $\hat{x}_{OL,n}$ estimation mismatch results from the process noise w_n that is not attenuated in the open loop estimation (as opposed to the closed-loop estimation in equation (4)). However, the fault $f_{S,n}$ does not influence the state estimate in any way. The residual is proportional to the state estimation error ($C_n x_n - \hat{C}_{OL,n}\hat{x}_{OL,n}$), the measurement noise v_n and the fault magnitude $f_{S,n}$. Note, that the negative effect of the state estimation error $C_n x_n - \hat{C}_n \hat{x}_n$ present in (5) has been eliminated in (7).

$$r_{OL,i,n} = C_n x_n - \hat{C}_{OL,n}\hat{x}_{OL,n} + f_{S,n} + v_n \quad (7)$$

The residual for the pressure sensor fault is presented in Fig. 2. This shows the simulated data for the transient conditions.

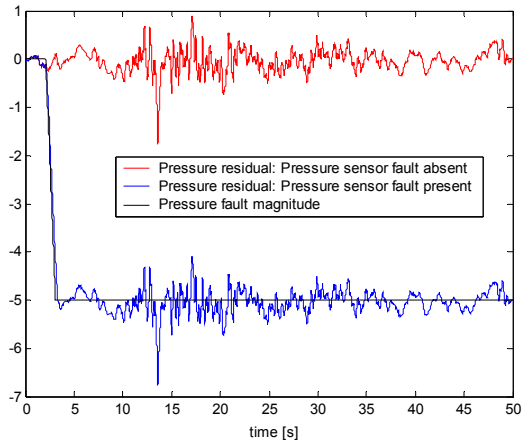

Fig. 2: Pressure measurement residual – open-loop estimator

The corresponding simulation results for temperature sensor fault residual are shown in Fig. 3.

C. The intake manifold leak directional residual generation

The intake manifold leak residual is generated by the non-linear fault detection filter presented in [9]. The dynamic observer is formulated in the following form. Note that system matrices denoted as time varying depend on the current state estimate.

$$\hat{\hat{x}}_{n+1} = A_n\hat{\hat{x}}_n + B_n u_n + \begin{bmatrix} K_{UIKF,n} & W_n \end{bmatrix} \begin{bmatrix} \Sigma_n \\ \mathrm{T}_n \end{bmatrix} \left(y_n - \hat{\hat{y}}_n\right) \quad (8)$$

$$\hat{\hat{y}}_n = C_n\hat{\hat{x}}_n$$

where $K_{UIKF,n}$ is the filter gain and W_n is the matrix that propagates the effect of faults/unmeasured inputs into the next time instant.

Additionally, two matrix coefficients T_n and Σ_n are introduced with the following properties:

$$\begin{bmatrix} \hat{q}_n \\ \hat{f}_{leak,n} \end{bmatrix} = \begin{bmatrix} \Sigma_n \\ \mathrm{T}_n \end{bmatrix} \left(y_n - \hat{\hat{y}}_n\right) \quad (9)$$

where $\hat{f}_{leak,n}$ is the leak directional residual and $\hat{q}_n$ are residuals decoupled from the faults/unmeasured inputs used for the process/measurement noise attenuation. Details of how the matrices T_n and Σ_n are computed may be found in [9]. The leak estimator shown in Fig. 1 is a part of the overall system. The filter (equations (8) and (9)) generates the directional residual that is sensitive to the leak ($\hat{f}_{leak,n}$). The intake manifold leak directional residual is shown in Fig. 4.

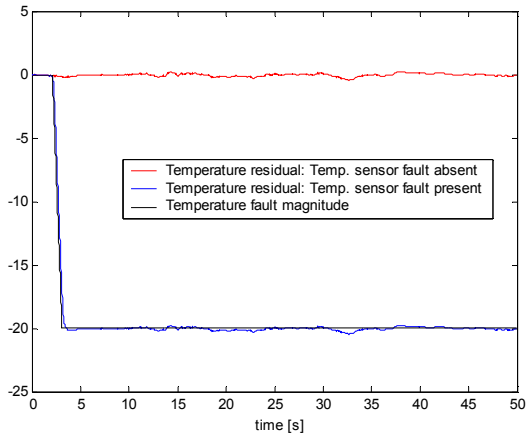

Fig. 3: Temperature measurement residual – open-loop estimator

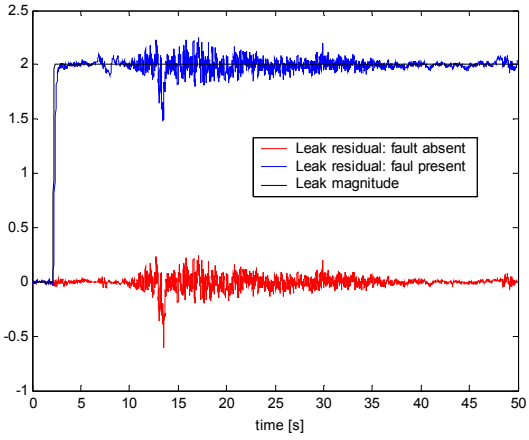

Fig. 4: The intake manifold leak directional residual

The remaining estimator residuals decoupled from the fault are shown in Fig. 5 ($\hat{q}_n$). The decoupled residuals facilitate the unbiased estimation and the attenuation of the process and the measurement noise.

In its fundamental form, the leak estimation is carried out under the assumption that output (sensor) faults are not

present in the system. A method for separating the influence of sensor and system faults will be described in the next section.

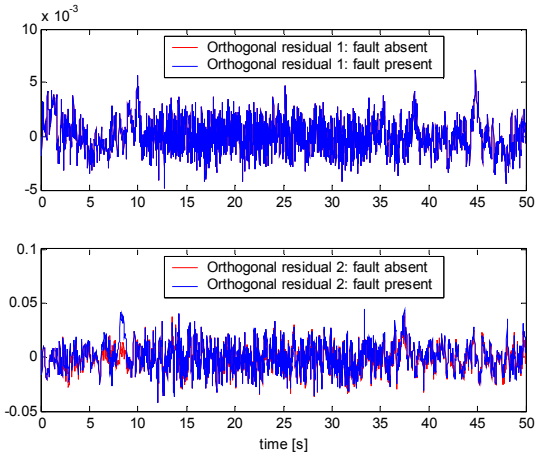

Fig. 5: The intake manifold leak decoupled residuals

D. Dedicated estimators sensitivity to other faults

In the analysis, the sensor faults residuals were generated for the assumption that the leak is not present in the system. A similar assumption about the sensor faults was made for the leak directional residual generation. It is important to assess the impact of the leakage on the pressure and temperature sensor residuals. Also, in the design of the fault detection logic, the intake manifold leak directional residual response to the pressure and temperature fault is important. As an example, the response of the temperature and pressure residuals to the intake manifold leak is shown in Fig. 6 and Fig. 7, respectively.

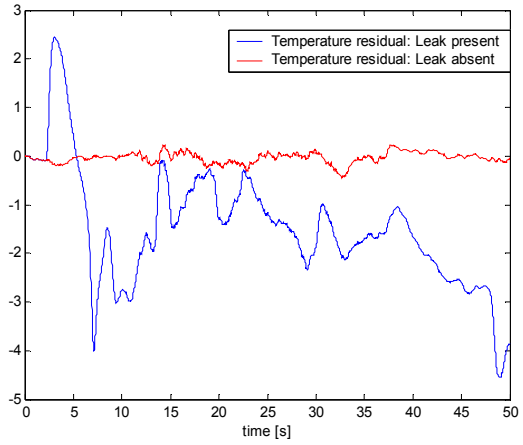

Fig. 6: Temperature residual response to the leak – the open-loop observer

It may be noted that the leak entails the change in the level of pressure and temperature residuals. It is important to notice that the levels for these residuals vary with the operating conditions. It is clear that for the intake manifold it may be difficult to detect the leak when the throttle is wide-open. Depending on the extent of the leak, the influence of such fault may however be negligible. In such a situation, the fault detection may not be critical.

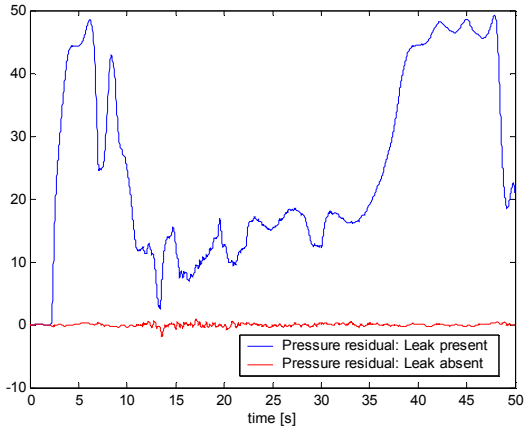

Fig. 7: Pressure residual response to the leak – open-loop observer

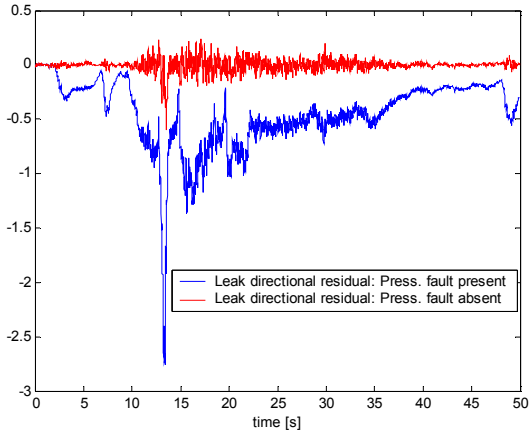

Fig. 8: Leak directional residual resulting from the pressure sensor fault

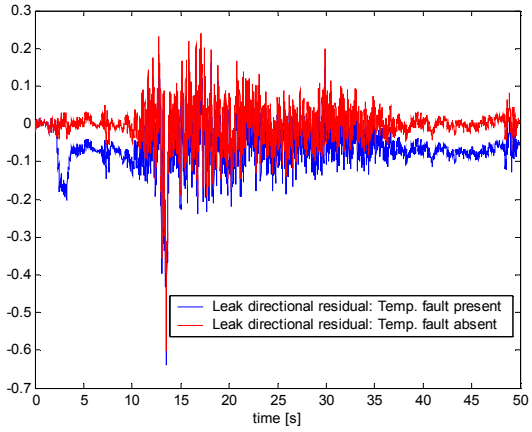

Fig. 9: Leak directional residual resulting from the temperature sensor fault

The leak directional residuals are affected by the sensor faults since the pressure and temperature measurements are used by the leak estimator. An example of how the pressure

sensor fault impacts the leak directional residual is shown in Fig. 8. For the temperature sensor fault, the leak directional residual is plotted in Fig. 9. It should be noticed that the leak residual strongly relies on the pressure sensor information. This is due to a lower fault detectability index for this output. The temperature sensor fault, however, results in a significantly lower residual change.

III. Determination of the Thresholds

Residuals generation is the first step in fault detection. For fault-free stochastic or uncertain systems, residuals are non-zero and therefore the threshold for the residuals must be established. If the residuals are within pre-defined limits, the system is assumed to be fault-free. Residuals exceeding the thresholds indicate possible faults in the system. It is important to define thresholds in a way that the system noise or uncertainty does not trigger the false alarm or system reconfiguration. In practice, thresholds should be based on the information about the extreme values for the fault-free system. A formal analytical derivation of the thresholds for a complex system, such as the intake manifold may not be possible. Additionally, the thresholds so estimated may also be too conservative if a multiple-model approach or the worst-case analysis is used.

In the work presented in this paper, thresholds are determined based on analysis of the real vehicle data compared with the model. An analysis of a number of FTP datasets provided the thresholds for fault-free conditions (a part of that data is shown in Fig. 10). The safety margin was also included to improve the design robustness.

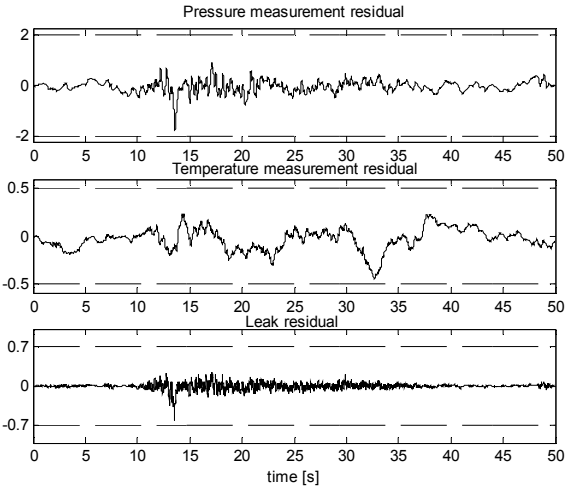

Fig. 10: Fault-free residual trace for thresholds determination

For the pressure sensor residuals, the threshold of $\pm 2\left[kPa\right]$ was determined. For the temperature sensor residual the threshold is set to $\pm 0.5\left[K\right]$. The intake manifold leak residual in Fig. 4 is assumed to stay within the range $\pm 0.7\left[\sqrt{N \cdot m \cdot g}/s \cdot kPa\right]$ for the fault-free system. The fault in the system will be detected when the value of any of the residuals violate the above threshold levels.

IV. Fault Isolation and Identification

The faults occurring in the system result in residuals violating the thresholds. The threshold violation indicates that the fault is present in the system but does not locate the fault. The fault isolation method based on the generalized observer scheme uses the table with the 'fault signatures' [10]. The pressure sensor fault causes its dedicated residual to violate the threshold but the temperature sensor residual remains unchanged. The temperature sensor fault moves the residual over the threshold while the pressure sensor residual remains within the usual limits. The intake manifold leak results in the pressure sensor and temperature sensor directional residuals moving over the thresholds. The fault signatures table is extracted from the analysis of the residuals behavior presented in section II. Note that the leak directional residual does not provide much information for the fault isolation system. The logical value of 1 denotes that the threshold is violated, 0 denotes that the residual is within the limits. The 'X' value denotes that either 0 or 1 is possible.

	Pressure sensor fault	Temp. sensor fault	Intake manifold leak
Pressure directional residual over threshold	1	0	1
Temperature directional residual over threshold	0	1	1
Leak directional residual over threshold	X	X	1

Table 1: The fault signatures table

The fault isolation is carried out assuming that only one fault occurs at any time. Due to the intake manifold dynamic characteristics, the thresholds established for the pressure, temperature and leak directional residuals are not violated simultaneously. The timing is also influenced by the system noise and the driving pattern which interact with the fault detection system. The time window that allows the checking of the threshold violations must be established. For the 90° event-based sampling and the allowed fault detection lag, the number of events for the algorithm time window is established. To achieve good robustness properties, a 100-event window was selected. This results in a delay of 1.5 s at an engine speed of 1000 rpm or 0.3 s at 5000 rpm. This delay may be reduced in some cases with the method presented in the following *Section A*. An alternative robust method in *Section B* will rely on a statistical analysis with a wider window to increase the detection reliability.

A. Threshold-based method

The threshold-based fault isolation method relies upon Table 1 and uses Boolean logic to test for residuals. The logical test may be structured in a way that the fault isolation lag is reduced. The test must detect zeros that identify the type of the fault in Table 1. In the case of the intake manifold

leak, all three residuals violate the thresholds. If three threshold violations are detected, the presence of the leak in the manifold is concluded. If within the selected data analysis window, and by the end of the lag period, either of the residuals does cross the threshold, it will indicate that either the pressure or the temperature fault is present. This concludes the fault isolation procedure. The example simulation results for the fault detection and isolation are shown in the sequel.

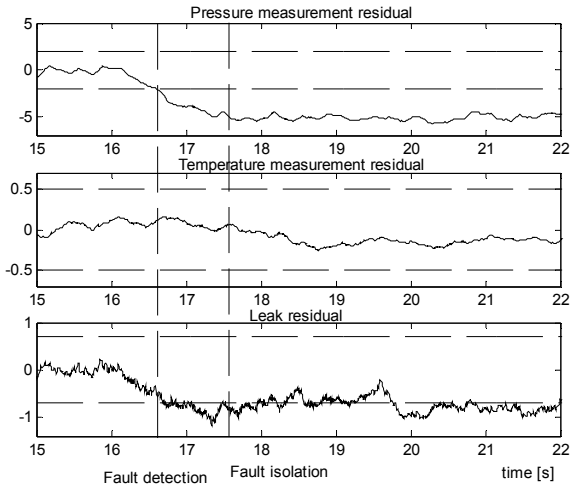

Fig. 11: The pressure sensor fault isolation

The pressure sensor fault detection is shown in Fig. 11. The pressure sensor fault in the system is detected when its directional residual (and only this residual) moves outside the thresholds. The violation of a pressure residual threshold is also possible by the manifold leak. However, the leak will also impact the temperature residuals. There is a need for some wait-time for the fault to propagate. Therefore a window of 100 events is assumed for this purpose. For the pressure sensor fault, the temperature residual should not cross its threshold. This does not happen within the window, providing the signature of the pressure sensor fault, and therefore the fault isolation is complete.

The case for the temperature sensor fault detection is shown in Fig. 12. In a similar way to the pressure sensor, the fault is first detected and then isolated. The fault signature reveals the temperature sensor fault. The intake manifold leak isolation is shown in Fig. 13. The procedure is clearly faster than the same for the sensor fault isolation. The fault isolation time event is characterized by the moment when all directional residuals cross over their thresholds.

B. Threshold method with statistical and expert analysis

Fault isolation methods may be enhanced by the incorporation of system-specific knowledge and a statistical analysis of results. For example, system knowledge with respect to the pressure sensor faults may be used. The fault detection is triggered by the pressure sensor and the leak directional residuals violating the thresholds. The leak residual violating the negative threshold immediately indicates that a pressure sensor fault has occurred. The leak, for a naturally aspirated engine, can only be positive. If the leak directional residual is found to be negative immediate fault isolation is possible. The pressure sensor fault isolation shown in Fig. 11 may be completed much quicker (i.e. within 0.1 [s] after the fault detection).

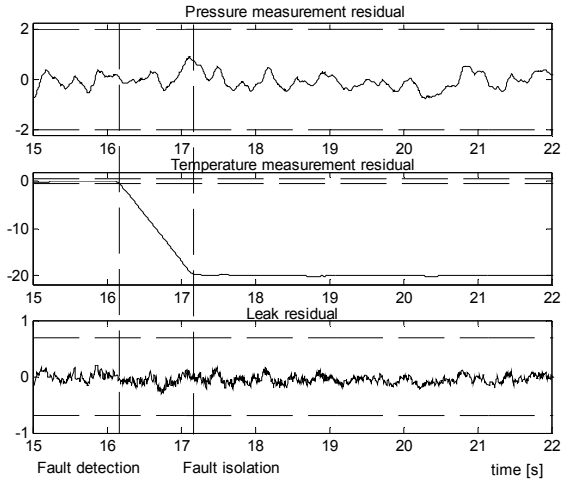

Fig. 12: The temperature sensor fault isolation

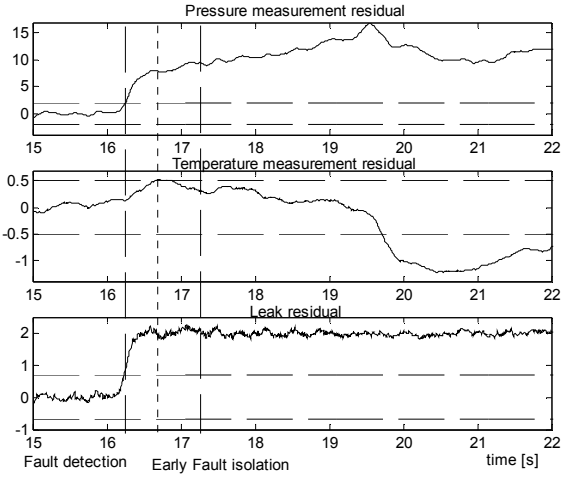

Fig. 13: The intake manifold leak fault isolation

To test the fault detection efficiency the following test was carried out. Faults are injected at different points of the driving cycle. The pressure sensor fault $f_{P_{im},n}$ and the temperature fault $f_{T_{im,meas},n}$ were modeled as drifts that saturate after 1 second at a level of +5kPa and -20°K, respectively. Note that during this test the pressure sensor fault is simulated with positive values to avoid trivial detection when the leak residual becomes negative. The intake manifold leak appears in a more abrupt way and is modeled as a drift signal that saturates after 0.2s at a level of 2 $\left[\sqrt{N\cdot m\cdot g}/s\cdot kPa\right]$. In this work only one fault magnitude level is considered. It may however be argued that the higher level of faults would result in higher value of residuals and consequently more reliable detection. The opposite situation, where the extent of the fault is less significant, is in fact more likely to impair the ability to detect these events. The fault detection speed is shown in Fig. 14. The time required for the detection of the

pressure and temperature faults is determined by the time when residuals cross over the thresholds and the window width (i.e. 100 events). Due to non-linearities, the initial fault isolation algorithm fails to detect the leak for faults which start to at 15.1 s and 20.1 s. This is due to the fact that within the test window, the temperature residual did not cross the threshold. Similar problems have been reported by other authors [6] for the intake manifold fault isolation.

A more robust method presented here aims to improve the fault isolation accuracy by the reasonable assumption that the leak area and the discharge coefficient of the leak source are constant. The variance of the leak directional residual is monitored to help isolate the fault more reliably. For the statistical analysis, the number of data points determines the accuracy. As a result, the window length is increased to 200 events. Within the 200-event window from the moment of the fault detection (see Fig. 13), the temperature directional residual only marginally violates the threshold. If the temperature did not violate the threshold within the data window, the pressure sensor fault would be isolated. Such a situation is shown in Fig. 14 for the leak occurring at time 15.1 s where the pressure sensor fault was isolated wrongly.

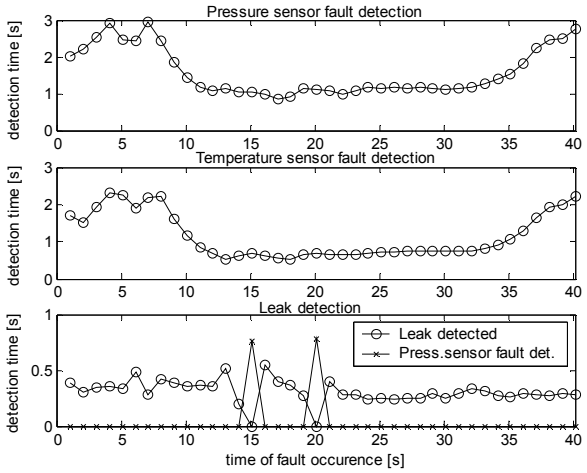

Fig. 14: Fault detection efficiency: simple threshold method

The monitoring of the variance of the leak directional residual will however improve the robustness. The leak directional residual that represents the leak area is assumed constant. It is then possible to establish the upper bound of this parameter. The upper bound for the variance of the leak residual based on the data analysis for the FTP cycles was determined to be 0.04. If the variance of the leak remains below its maximum value, it indicates that there might be a leak in the intake manifold. The data window is shifted forward in time until the temperature residual violates the threshold which indicating the leak, or until the variance violates its threshold indicating the pressure sensor fault.

The fault isolation logic is formulated in Table 2. The improved robustness of the method is presented in Fig. 15. It should be noted that the robustness of the method comes at the expense of the speed of isolation.

Accurate fault isolation is important for the control system re-configuration. For the re-configuration, the identification of the fault extent is essential. The fault identification is only required for the intake manifold leak. The directional residual estimate $\hat{f}_{leak,n}$ provided by the process fault detection filter is used for this purpose. The residual is a combination of the product of the leak discharge coefficient, the leak area estimate and the noise. Since the fault $f_{leak,n}$ is assumed to be constant and the noise is filtered out, the leak estimate may therefore be used by the control algorithm.

	Pressure sensor fault	Temp. sensor fault	Intake manifold leak	Extend the data window
Pressure directional residual over threshold	1	0	1	1
Temperature directional residual over threshold	0	1	1	0
Leak directional residual over threshold	X	X	1	1
Leak directional residual variance over threshold	1	X	0	0

Table 2: Extended fault signatures table

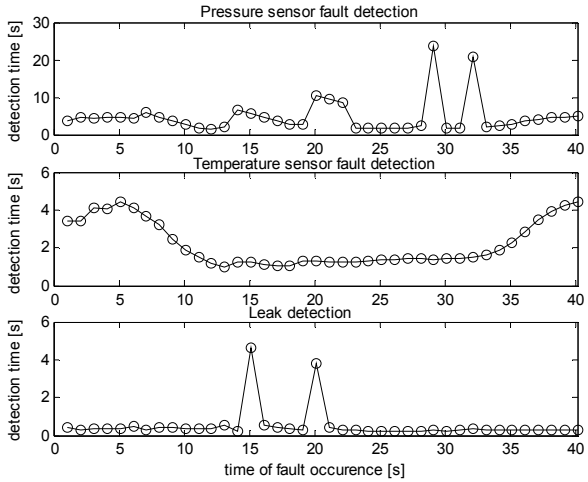

Fig. 15: Robust isolation of the intake manifold faults

V. CONCLUSION

For a vehicle emissions control system, continuous monitoring of the engine variables to ensure proper functioning is critical. Typical faults were considered associated with the intake manifold sensors and systemic faults such as the presence of leakage in the intake manifold were exploited to develop reliable methods for fast detection and isolation of the faults.

The results presented in the paper use system inputs and external variables such as engine speed and ambient conditions from the real vehicle. The intake manifold subsystem is simulated by a non-linear event-based discrete time model.

The proposed fault detection and isolation method performs threshold tests on the directional residuals. The residuals are

generated by a combination of a state-dependent Kalman filter, an open-loop observer and an unknown input estimator. The use of the state-dependent Kalman filter is unusual and appears promising. An interesting conclusion is that the open-loop observer is more effective than the closed-loop observer for the non-linear system under consideration here. The proposed fault detection was followed by an isolation strategy. Due to the presence of the unknown input estimator, the fault magnitude is also estimated. This will also enable its use for the fault compensation. To increase robustness, a fault signature diagnosis algorithm was proposed that will be triggered by the fault detection mechanism.

In this approach, a set of measurements over a fixed period of time was made and the properties of the residuals analyzed. A fault isolation enhancement was also proposed which involves the introduction of the residual statistical analysis. For this purpose, the variance of the leak residual signal was monitored. Additionally, the system-specific knowledge was incorporated which has improved the robustness of the fault detection algorithm. It was demonstrated that all the three types of faults can be safely detected and isolated when the detection window is of a proper size. The trade-offs between the precision of detection and the speed of detection has also been emphasized.

ACKNOWLEDGMENT

We would like to thank Dr. Man-Feng Chang of GM R&D for many useful discussions and his kind support of the research project.

REFERENCES

[1] Cho, D., P. Paolella. “Model-based failure detection and isolation of automotive powertrain systems”, Proceedings of the American Control Conference, San Diego, California, USA, 1990

[2] Rizzoni, G., P. M. Azzoni, G. Minelli. “On-board diagnosis of emission control system malfunctions in electronically controlled spark ignition engines”, Proceedings of the American Control Conference, San Francisco, USA, 1993

[3] Gertler, J., M. Costin, X. Fang, Z. Hira. “Model based diagnosis for automotive engines – algorithm development and testing on a production vehicle”, IEEE Transactions on Control Systems Technology, vol. 3, no. 1, pp 61-69, 1995

[4] Kimmich, F., A. Schwarte, R. Isermann. “Fault detection for modern Diesel engines using signal- and process model-based methods”, Control Engineering Practice, vol. 13, pp. 189-203, 2005

[5] Nyberg, M. *Model Based Fault Diagnosis: Methods, Theory, and Automotive Engine Applications*, Linköping University, PhD thesis No. 591, 1999

[6] Nyberg, M. “Model-based diagnosis of an automotive engine using several types of fault models”, IEEE Transaction on Control Systems Technology, 10, 5, pp. 679-689, 2002

[7] Dutka, A., H. Javaherian, M. Grimble, “Model-Based Nonlinear Multivariable Engine Control”, Proceedings of the American Control Conference, pp. 3671-3677, New York, NY, USA, 2007

[8] Dutka, A., H. Javaherian, M. Grimble, “State-dependent Kalman filters for robust engine control”, Proceedings of the American Control Conference 2006, Minneapolis, Minnesota, USA

[9] Giovanini, L and A. Dutka. “Fault Isolation Filter for Nonlinear Systems”, IFAC Safeprocess 2003, Washington, USA, 2003

[10] Simani, S., C. Fantuzzi, J. R. Patton. *Model-based Fault Diagnosis in Dynamic Systems Using Identification Techniques*, Springer-Verlag London, 2002